

# Optimisation of Operating High Voltage of the large area Resistive Plate Chamber for ICAL experiment

---

S. Pethuraj,<sup>a,1</sup> G. Majumder,<sup>a</sup> K.C. Ravindran,<sup>a</sup> B. Satyanarayana,<sup>a</sup> Umesh L<sup>a,b</sup>

<sup>a</sup>*Tata Institute of Fundamental Research,  
Mumbai-400005, India*

<sup>b</sup>*The American College,  
Madurai-625002, India*

E-mail: [s.pethuraj@tifr.res.in](mailto:s.pethuraj@tifr.res.in)

**ABSTRACT:** The Resistive Plate Chamber is a widely used detector in high energy physics. The operating potential of this chamber is determined by the optimisation of the efficiency and noise rate of the device. This optimisation is based on the assumption that the performance of the device over the whole surface area is uniform. The INO-ICAL experiment is going to use  $\sim 30000$  RPC of size  $\sim 2\text{ m} \times 2\text{ m}$ . All the RPC will have to pass a minimum quality assurance criteria, but may not be able to maintain a good uniformity over the whole surface area, particularly for the whole running period of about twenty years. This paper describes the choice of the optimum operating HV for an RPC of non-uniform response.

**KEYWORDS:** RPC, Gaseous detectors, Charge induction, Neutrino detectors

---

<sup>1</sup>Corresponding author.

---

## Contents

<b>1</b>	<b>Introduction</b>	<b>1</b>
<b>2</b>	<b>Experimental Setup</b>	<b>2</b>
<b>3</b>	<b>Data Analysis</b>	<b>3</b>
<b>4</b>	<b>Efficiency Plateau of the RPC detectors</b>	<b>5</b>
<b>5</b>	<b>Pixel-wise efficiency and Strip Multiplicity for different HV</b>	<b>6</b>
<b>6</b>	<b>Efficiency using Selected Events</b>	<b>9</b>
<b>7</b>	<b>Position and Time resolution of the RPCs</b>	<b>9</b>
<b>8</b>	<b>Conclusion</b>	<b>12</b>

---

## 1 Introduction

The proposed India-based Neutrino Observatory (INO) at Bodi hill ( $9^{\circ}58'N$ ,  $77^{\circ}16'E$ ) in the Southern part of India, with at least 1 km rock overburden in all directions will be the largest experimental facility of basic science in India to carry out front-ranking experiments in the field of particle and astroparticle physics. The Iron Calorimeter (ICAL) detector is the proposed underground neutrino physics experiment in the INO cavern, which aims to observe the neutrino oscillation pattern at least over one full period. Main goals of this experiment are the precise measurements of neutrino oscillation parameters including the sign of the 2-3 mass-squared difference,  $\Delta m_{32}^2 (= m_3^2 - m_2^2)$  through matter effects, and, last but not the least, the search for any non-standard effect beyond neutrino oscillations [1]. The detector size is  $48\text{ m} \times 16\text{ m} \times 14.5\text{ m}$  made of 151 layers of 5.6 cm iron plates interleaved with the Resistive Plate Chamber (RPC) for the detection of the muon trajectory. There will be  $\sim 30000$  RPCs of size  $\sim 2\text{ m} \times 2\text{ m}$ , made of glass gap with pickup panels and corresponding electronics to collect and store the induced signals which are produced due to the avalanche of electrons along the trajectory of the charged particles. Initially, a small number of this large RPC [2] were built in the laboratory in collaboration with the industry. After establishing the whole procedure, jobs are given to different industries, e.g., production of the gas gap, pickup panel, electronics, power supply etc., are given in different companies. After assuring the quality control (QC) of each component separately, all are brought back to the laboratory for final assembly and test the performance of the RPC. Though there is a stringent condition on the QC at the vendor's place, the performance of the finally produced RPC is slightly worse than the earlier produced RPC in the laboratory. One example is the uniformity of the gas gap and consequently the variation of gain/noise rate of RPC as a function of the position in the RPC. To have a higher gain of the RPC

in the whole surface area, the noise rate, as well as the probability of streamer formation, is also increased in the high gain area of the detector, which eventually deteriorates the position and timing performance of the RPC detector. The optimal choice of the applied HV is obtained by considering the efficiency and resolutions. The outline of the paper is the following. Section 2 describes the experimental setup. Data analysis techniques are described in Section 3. Section 4 shows the overall efficiency of a poor quality RPC as a function of HV and the V-I curve of the detector. Section 5 discusses the response of the RPC in different regions of the detector area. The overall efficiency is calculated based on the optimum selection criteria explained in Section 6. The section 7 shows the position and time resolution as a function of HV and finally we conclude our findings in section 8.

## 2 Experimental Setup

RPCs were introduced in the 1980s in the particle physics experiments as a replacement for spark counters. Due to its rugged structure and its large area coverage with uncompromised efficiency and time resolution made it a significant element in the High Energy Physics as Trigger detector and Time-of-Flight detector in various experiments. The operation of the RPCs are based on the detection of the gas ionization produced by the charged particle when it passes through the active area of the gaseous chamber and subsequently the avalanche due to the strong electric field in that region. The RPCs used as trigger detectors have a gas gap in the order of a few mm. If the RPCs are used in the Time of Flight (ToF), the gap in the order of a few 100  $\mu\text{m}$  used to get the better time resolution (few 10 of ps). The gas mixture along with an operating voltage decides the working mode of the detector whether it is an avalanche or streamer. In avalanche mode, the electron multiplication occurs due to the drifting and collision of the electrons with gas molecules. The avalanche became the precursor of the new process called streamer if the electron multiplication reaches the extreme value [3, 4]. In the Streamer phase, the kinetic energy of the electron is low and the recombination of the electron-ion results in the photons and this create delayed secondary avalanches with respect to the first one. If the number of photons are large enough and the applied electric potential is strong enough will produce a large number of the secondary avalanches until the local density and electron-ion distributions are such to create a plasma between two electrodes (electron and ion distribution connects the two electrodes). In this process, the extremely high current such as 100 time larger than the avalanche is flown through the gas gap, until the electrons and ions are collected by the electrode.

The RPCs used in this study are made by placing two thin glass plates of 3 mm thickness, 2 mm apart from each other. The gap between the two glass plates is maintained to be 2 mm using poly-carbonate "button" spacers. The sides are sealed with side spacers to form a closed chamber. There are gas inlet and outlet nozzles at the corners of the chamber through which the mixed gas is flown. The outer surfaces of the glass chamber are coated with a thin film of graphite paint for the application of external high voltage. The resistivity of the coat is chosen by optimising the application of uniform electric field in the gap as well as localising the induced signal in a small area. A thin layer (50  $\mu\text{m}$ ) of insulated mylar sheet is kept in between the chamber and pickup panels on both sides. The pickup panels are made of the copper strips with a width of 2.8 cm and an inter-strip gap of 0.2 cm pasted on the plastic honeycomb material, where the other side is pasted with a thin aluminium layer for grounding. The RPCs are operational in avalanche mode

with a non-flammable gas mixture of  $C_2H_2F_4$  (95.2%), iso- $C_4H_{10}$  (4.5%) and  $SF_6$  (0.3%), which are continuously flown through the gas gap with a rate of 6SCCM per RPC.

To work on the RPCs in avalanche mode, the major component of the gas mixture is the electronegative freon gas ( $C_2H_2F_4$ ) with enough primary ionization production along with that low pathlength for the electron capture. Due to the electronegative property of the gas, it controls the electron multiplication within the Meek limit [3, 4]. The iso- $C_4H_{10}$  is the polyatomic gas, which has high absorption probability for the UV photons produced in the electron-ion recombination. The absorbed energy is dissipated as the rotational-vibrational energy levels. The third gas  $SF_6$  is used with minimal volume fraction but it plays a dominant role in operating the RPCs in the avalanche mode by quenching the electrons.

Few RPCs with a large non-uniformity in terms of efficiency and noise are studied to find the optimum operating HV. There are many sources of the non-uniformity, e.g., uniformity of the thickness of the glasses & supporting spacers to maintain the gas gap, resistivity in the graphite coating, flatness of the pickup panels, difference in the gain of amplifiers as well as the threshold of the discriminators, the characteristic impedance of the pickup strips due to variation of width as well as depth of the supporting material etc.

RPCs are tested using the existing 85 ton miniICAL experimental setup [5], which is a miniature version of ICAL and a schematic view is shown in figure 1. In absence of easily available test beam facilities with muon beams, the miniICAL is used to trigger cosmic muon trajectory. Though the miniICAL performance is being tested with the 1.4 T magnetic field, this study used the data collected without any magnetic field. Also, there are 20 RPC (two RPC in a gap with 10 RPC in a vertical column) in the system, but this study is based on 10 RPC of a column <sup>1</sup>.

The characteristic impedance of the strip is around  $\sim 50 \Omega$ . The readout strips are placed orthogonally on either side of the RPC to measure the position of the traversed charged particle (X-coordinate from the bottom strip and Y-coordinate from the top strip plane). The induced signals due to the avalanche multiplication inside the RPC are amplified and discriminated by an 8-channel NINO ASIC chip [6]. The LVDS output of NINO is fed to the FPGA based RPC DAQ system. Finally the electronic outputs of an RPC are 128 logic units, to identify the induced signal in the strips and sixteen time measurements. The 128 logic unit is defined as hit<sup>2</sup> and used to localise the position of the traversing charged particle. For the time measurement, every 8<sup>th</sup> strip are connected together to have a single output of 8 strips.

This study is performed using cosmic muon events, which are triggered by the coincidence of signals in four fixed RPCs in that column with the time window of 100 ns. The logical “AND” is done for X- and Y-plane independently to form the trigger signals from X- and Y-plane. The final trigger is created by logical “OR” of the trigger signals from X- and Y-plane.

### 3 Data Analysis

One of the main disadvantages of this setup is the uncertainty of the position and time measurement of muon trajectories in the test RPC. In test beam setup, muon position is measured with the tracking

---

<sup>1</sup>The numbering of RPCs starts from the bottom and the top layer is numbered as 9.

<sup>2</sup>Induced signal in a strip larger than 100 fC.



**Figure 1.** A view of 85 ton miniICAL detector with 10 layers of RPC detector.

device of position resolution about  $\sim$ mm or less and time is measured very precisely from the beam delivery system [7]. In this setup, those are measured in a crude way.

The typical noise rate of a strip is  $\sim$ 100 Hz at 10 kV. The four-fold coincidence logic reduces the events triggered by the random coincidence of noise. But, muon is contaminated by the correlated electronic noise as well as cosmic showers mainly due to interactions of remaining hadrons of cosmic ray particles on the roof of the building and the iron in miniICAL.

Most of the analysis framework is done independently using the information in X-strips and Y-strips of different layers independently and then combined together to localise the position of the muon in two dimensional space in an RPC.

The muon position in the RPC is simply the mean of the strip positions in the RPC. For the timing measurement, strips with an earlier timestamp amongst different strips are used as the measured time for that layer. To remove the background events, each layer is considered only when there are at most three hits in a plane and all three hits should be in consecutive strips. This criterion is used also to reduce the small fraction of streamer pulse. Position resolution of an RPC is drastically deteriorated with the multiplicity 4 or more [8] and will be discussed more in section 5.

The position alignment of an RPC with respect to the remaining system is done through an iterative procedure, where the muon trajectory is fitted with a simple straight-line equation using the information of all other detectors. The test layer is aligned by comparing the measured position in that layer with respect to the extrapolated position from the fit using other layers. This entire process is repeated iteratively where residual distributions of positions are corrected and updated for all layers. The details of the alignment technique are given in [9] and the same iterative procedure is also used for the correction of time offset, but for the timing in a layer there are sixty-four offset

corrections (for each and every individual strip) per plane.

After all these criteria, straight lines for the muon are fitted in both X-Z plane and Y-Z plane independently. Each fit must contain at least six layers and  $\chi^2/ndf$  is less than two are considered for further study. Applying these conditions simultaneously on both X-Z and Y-Z plan select almost 100% pure muon signal in the event. Using the fit parameters, muon trajectories are extrapolated to the test RPC. The position resolution of the RPC's are  $\sim 8$  mm [8]. Thus the error on the extrapolation on top of the miniICAL is also about  $\sim 6-7$  mm, but this is minimum in the middle layers, which is about  $\sim 3$  mm. Similarly, the uncertainty of the time measurement in each layer is  $\sim 1$  ns [10] and error on the extrapolated time at the top of miniICAL is 0.8-0.9 ns, whereas at the centre of the stack it is  $\sim 0.4$  ns. These extrapolated uncertainties on position and timing are larger than the typical values achieved in test beam facilities [11]. Measured position and time resolutions are convoluted with the error due to extrapolation, but for the comparison of the performance as a function of applied HV, the effect will be the same for all HV. The choice of optimum HV will not affect much with these extrapolated errors.

#### 4 Efficiency Plateau of the RPC detectors

During the preliminary testing of the RPC under the study, the first parameter is to measure the Voltage-Current characteristics of the RPC. The measured RPC count rate per strip and current at different HV is shown in Figs. 2(a) and (b) respectively. In general, the choice of the operating high voltage (HV) of the RPC detector is determined by the overall detection efficiency of the RPCs for the charged particle as a function of applied HV. The operating point (workingpoint) of the RPCs are decided by the “knee” voltage; the voltage at which the overall efficiency of the RPCs reached 95% of the maximum efficiency[12, 13]. The efficiency of the RPC discussed in this section is estimated for the pixel<sup>3</sup> when muon passes through the pixel. The size of the pixel is 3 cm, whereas the extrapolation error  $\sim 8$  mm, to incorporate the uncertainty of extrapolation, any hit in the RPC strips with the 3 cm from the extrapolated position is used for the efficiency measurement. Even with the disadvantage due to error in track extrapolation, there is also an advantage over test beam or conventional muon telescope. In general, the detection efficiency of the selected strips is estimated using the cosmic muon telescope made of scintillators as trigger detectors and RPCs as detectors under test. In that method, the performance of only a selected region of the RPC is studied. The same is true for test beam activities also. But to study the detailed (pixel-wise) performance of the RPC detectors over the whole area, the RPC detectors kept in miniICAL or any other RPC stack is certainly a better option. It was mentioned earlier that the uncertainty of the extrapolation is minimum in the middle of the stack, but due to other considerations, the HV scan measurement is performed for the RPC, which is kept in the 8th layer of the miniICAL. Muons events are collected with the in-situ trigger from the time coincidence of layers 2, 3, 4 and 6. In the different runs, the HV and all other conditions of all RPCs are kept the same except the HV of layer 8. The muon trajectory is fitted with the hit points of all layers excluding layer-8 and interpolated to layer-8 and matched with the measured hit position in that layer. The overall efficiency as a function of High Voltage for the RPC under observation is given Fig. 2(c). From the overall efficiency measurement

---

<sup>3</sup>Area of 3 cm $\times$ 3 cm in the RPC detector to match the strip pitch.



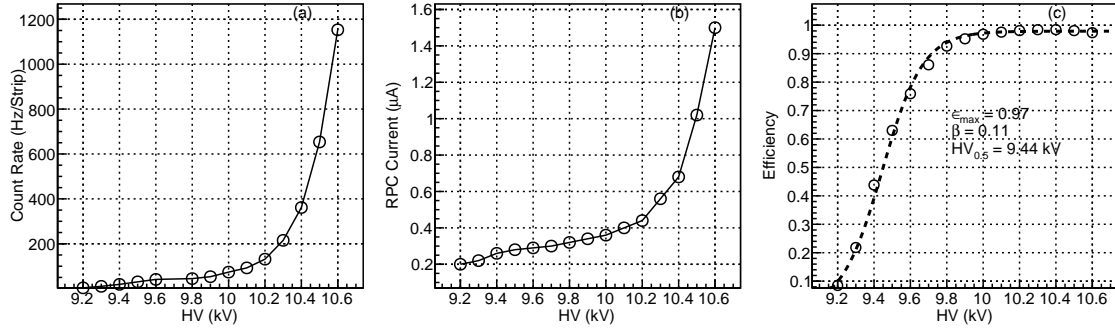


**Figure 2.** (a), (b) and (c) are average count rate per strip, the V-I curve and the measured efficiency vs high voltage for the RPC under observation.

it is observed that the efficiency of the RPC is saturated at around 10.2 kV of the applied high voltage. The efficiency as a function of the HV is fitted using the sigmoidal function is given in Eqn 4.14,

$$\epsilon = \frac{\epsilon_{max}}{1 + \exp[-(HV - HV_{0.5})/\beta]} \quad (4.1)$$

where  $\epsilon_{max}$  is the maximum efficiency as HV is  $\infty$ .  $HV_{0.5}$  is the HV value for which the efficiency is half of the maximum efficiency ( $\epsilon_{max}$ ).

## 5 Pixel-wise efficiency and Strip Multiplicity for different HV

Comparing the knee of the efficiency plots with other results, e.g., Ref. [7], the large difference is observed between the applied HV for the saturation in the efficiency and the 50% efficiency of the RPC. This behaviour might be due to the variation of gain in different regions of the RPC, where certain regions have larger gain and reach the maximum efficiency earlier than the regions with low gas gain. The figure 3(a) shows the pixel-wise combined efficiency of X&Y-side for the whole RPC at 9.4 kV. The three bands parallel to the Y-axis are due to the malfunction of electronics in the three strips. There are regions where efficiency is almost zero and some regions are more than 90% efficient. The efficiency will increase with applied HV, but to have saturated efficiency of these low gain regions, one needs a substantial increase of applied HV.

Depending on the efficiency in the RPC at 9.4 KV, the whole surface area of the RPC is divided in 10 zones, with efficiency, 2-10%, 10-20% and so on.

Along with the overall efficiency of the RPCs, the other parameter which tells about the behaviour of the RPC detectors is the cluster size or hit multiplicity distribution. The hit multiplicity distribution for the regions with efficiency of 20-30 % and 50-60 % at the applied voltage of 9.4 kV are shown in Figs.3(b) and (c). In general for a stable operational RPC, the strip multiplicity produced by avalanche due to the passage of the muon through RPC detector is upto three strips. The hit multiplicity beyond three and until  $\sim 20$  is mostly due to the hadronic shower and steamer development inside the gas gap. The events with strip multiplicity of more than  $\sim 20$  is due to

<sup>4</sup>The observed behaviour of the X- and Y-plane is similar. Thus the results from one of the planes is described in further sections.

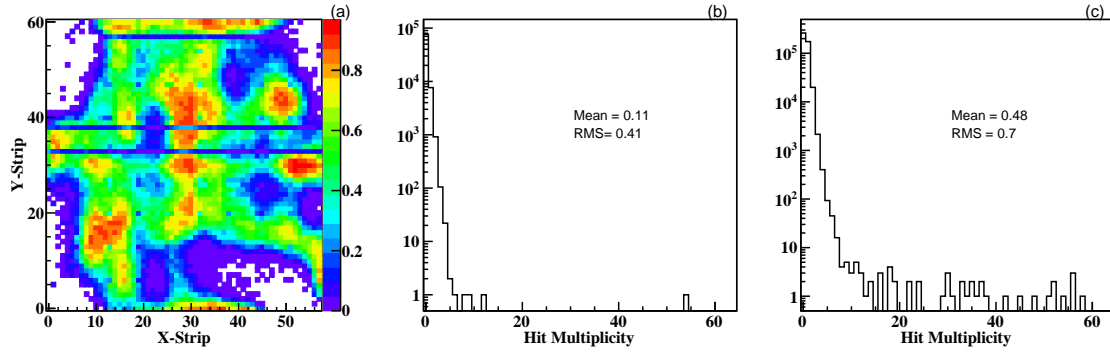


**Figure 3.** (a), (b) and (c) are the pixel-wise efficiencies and hit multiplicity distribution for efficiency zone 20-30 % and 50-60 % of the RPC at applied voltage of 9.4 kV.

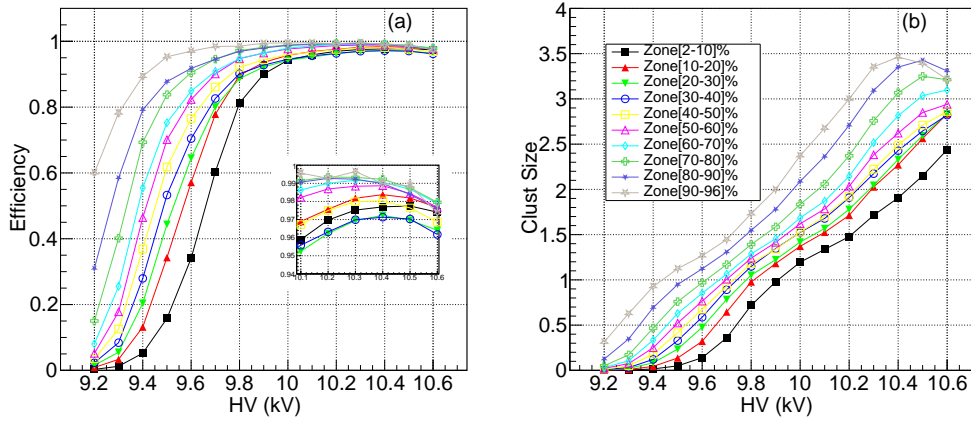


**Figure 4.** (a) and (b) are the measured efficiency and average cluster size vs high voltage for different zones of the test RPC.

electronic noise that occurred due to EMI from various sources around the experiment. But, there is no sharp boundary between the streamer and electronic noise. From the operational point of view, hit multiplicity increases with the applied HV.

The average efficiencies in one of the RPC planes at different HV for different zones are shown in the Fig. 4(a). It is clearer from the figure that the different zone reaches the saturated efficiency at different HV. The inset plot of Fig. 4(a) shows the decrease of efficiency at very high voltage, which is due to a visible dead time of the detector caused by the large noise rate. The average hit multiplicities (cluster size) for different HV at various efficiency zones are shown in Fig. 4(b). Similar to the efficiencies, the multiplicities are also a combined function of the zone and applied HV. It was mentioned earlier that one of the sources of high multiplicity is the streamer formation and it causes the deterioration of position resolution. Earlier studies [8] showed that the position resolution drastically deteriorates with the multiplicity of four or more. The operation of this RPC at 10.1 kV will have a large region with an average multiplicity of four or more and can not be used for any physics study, e.g., identification of trajectories and the accurate measurement of momentum due to poor position resolution. The position resolution for different hit multiplicities from one



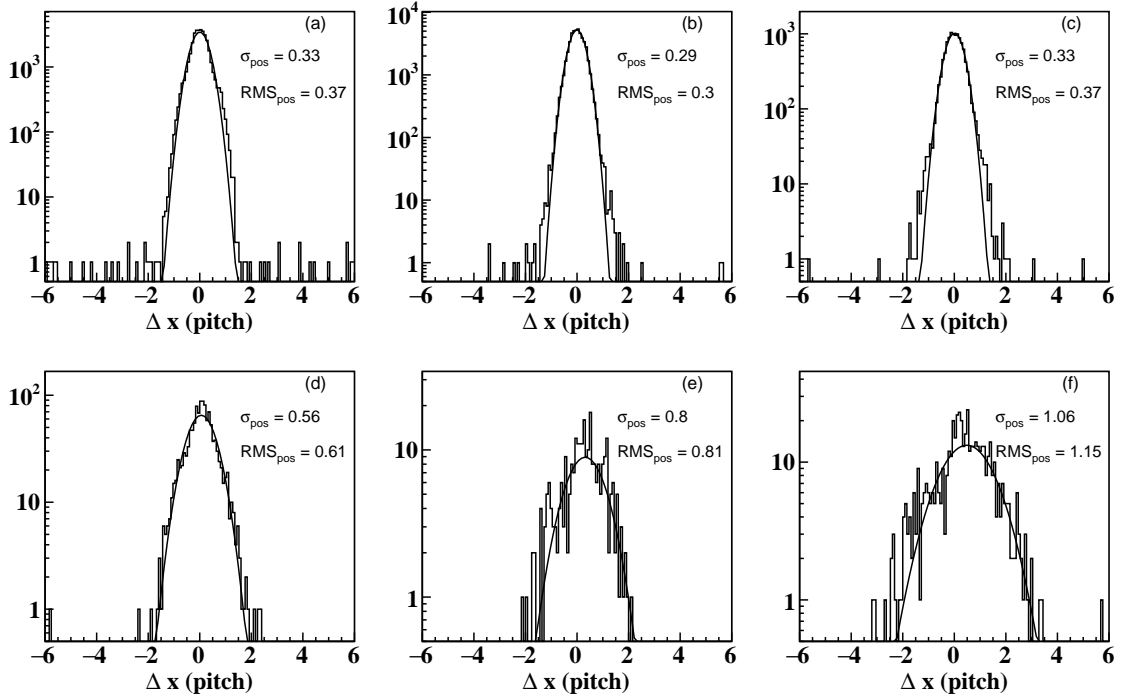


**Figure 5.** The measured position resolution of the observation layer for different multiplicity from (a) one to (e) five and (f) greater than four at the 60-70 % efficiency region.

to five and multiplicities greater than four hits for the observation RPC at 10.1 kV for efficiency region of 60-70 % are given in Figs. 5 (a) to (f). The observed position resolution for applied HV vs efficiency zones for different multiplicities (from one to five and greater than four) are given in Figs. 6 (a) to (f). Some regions are empty due to the omission of resolutions with a very low number of events.

At the low HV, events with larger multiplicities, e.g., three or more are dominated by noise and similarly at larger HV, events with low multiplicity are also dominated by noise associated with inefficiency of the detector. The multiplicity increases with HV for the whole surface area, but it is always less in the low-efficiency zone in comparison with higher efficiency zones at each high voltage. The lowest resolutions for each multiplicity, which is nearly diagonal points in these plots, are the regions of high purity signal. With high voltage there are relatively more events with a large avalanche pulse, thus resolution with multiplicity four is reduced with HV. Though the resolutions for multiplicity more than four are always larger than the events with multiplicity 1 to 3, except for multiplicity one with very high voltage. The larger resolution is mainly due to the contamination of streamer pulses. Similarly, for five-hit multiplicity, it is similar but happening at an even higher voltage. At larger HV, e.g., 10.6 V, events with multiplicity one is dominated by the region of dead strips and consequently observed large resolution. Overall, the observed position resolution for the events with four hits or more shows a substantial deterioration in comparison with the events with multiplicities upto three.

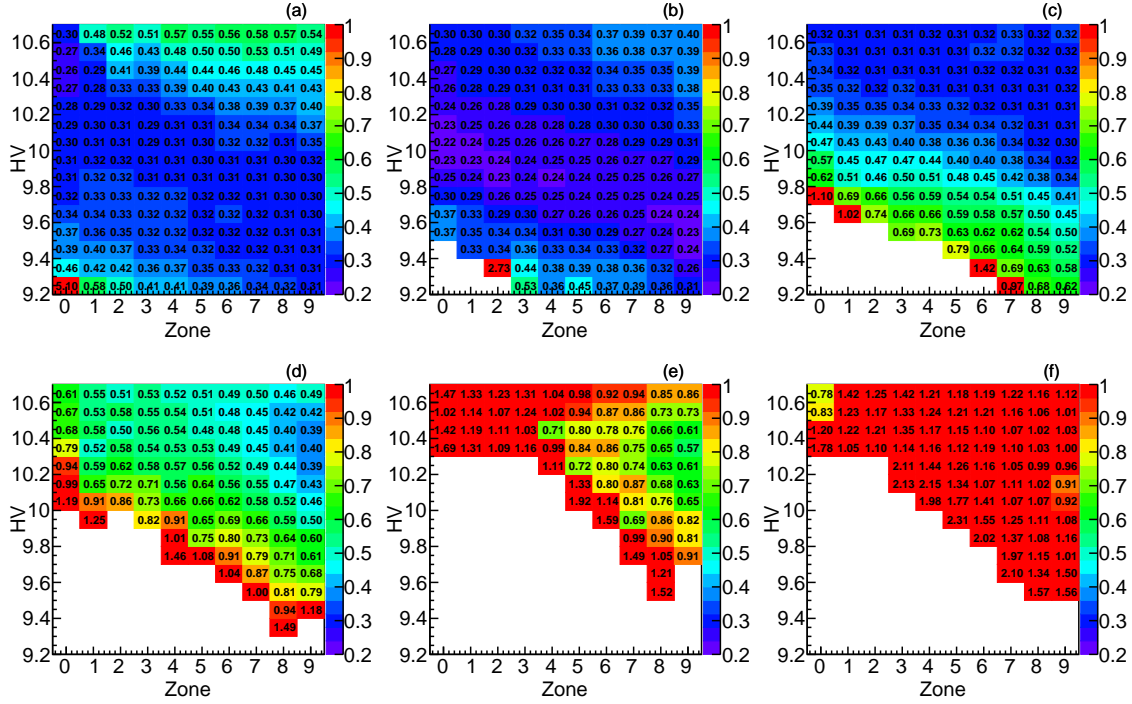


**Figure 6.** The measured position resolution of the observation layer for HV vs efficiency region for different multiplicity from (a) one to (e) five and (f) greater than four.

## 6 Efficiency using Selected Events

The efficiency of the RPC which was discussed in the section 4 is estimated without any selection criteria on the multiplicities, the event can have any number of hits in the RPC under the study. It was discussed in the previous section that the avalanche can induce upto  $\sim$  three strip hits and beyond that is not recommended to use for any physics study due to worse localisation of signal. Thus, the definition of the efficiency is modified with the criteria of accepting events with at most three consecutive hit in this test RPC. The average efficiencies of the selected events defined as selected efficiency for the whole detector as a function of applied voltage are shown in Fig. 7

The average efficiency has a peak at  $\sim$ 9.8-9.9 kV for the RPC under observation suggests that the optimum operating voltage of the RPC under the study should be 9.8-9.9 kV. Thus from the efficiency point of view, the optimum operating voltage of this RPC is less than 10.1 kV which was obtained earlier with the simple efficiency measurement. Beyond 10.1 kV, the efficiency of the selected events are decreasing because of the rejection of events with large multiplicities, mainly due to the formation of streamer pulses and it is more for high gain regions.

## 7 Position and Time resolution of the RPCs

The efficiency is not the only ultimate test for the optimisation of the applied HV. The position resolution drastically deteriorated for multiplicity four or more, but also these are worse for multiplicity three in comparison with multiplicity one or two. Even after rejecting the events with hit

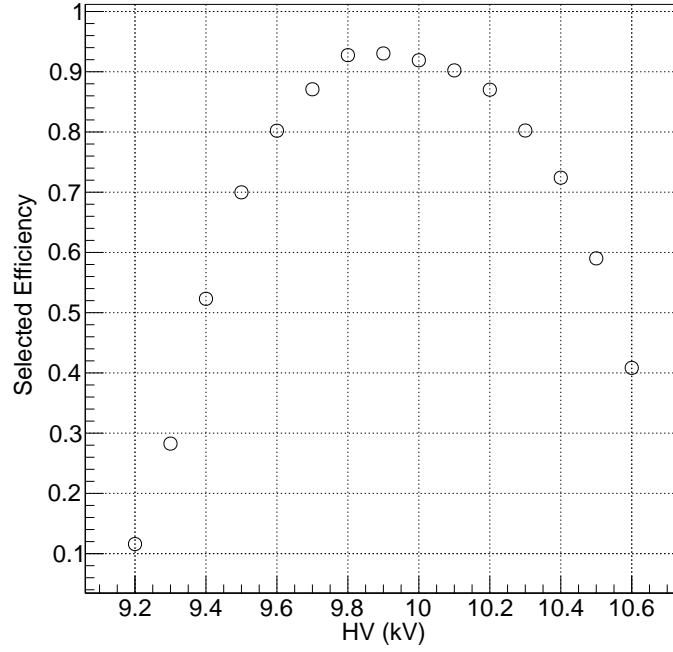


**Figure 7.** The measured efficiency from the selected events vs high voltage for the RPC under observation.

multiplicities four or more, the physics parameters can be affected bit by the hit multiplicity three. Until now the main parameter considered only the efficiency (with and without multiplicity criteria) to choose the operating voltage of the RPC. But to look at more detailed performance the physics parameters of the RPCs such as position and time resolution of the RPC are very important. The position residues, the difference between the observed and extrapolated positions are distributed and the resulting distribution follows the gaussian shape. The observed distribution is fitted with the Gaussian function the fitted  $\sigma_{pos}$  is considered as the position resolution of the RPC. Similar to the position resolution, the time resolution is also estimated by fitting the distribution of the difference between the observed and extrapolated time of the RPC layer. The distribution of position and time residues at 9.8 kV are shown in Figs. 8 (a) to (f) for different efficiency regions such as 20-30 %, 50-60 % and 80-90 %.

The position and time offsets calculated from the muon data recorded with different HV. The mean of the time residues (can be called avalanche delay with respect to the trigger signal) is expected to show the correlation with HV (which is calculated with the time corrections calculated using the data from 9.8 kV). As the HV increases the signal height increases at a faster speed, consequently the threshold crossing time for the avalanche signal is earliar with respect to the trigger signal. From Fig. 9(a), the avalanche delay vs HV is fitted using the straight-line upto 10.2 kV until there the linearity exists. The obtained slope for one of the planes is  $-7.51$  ns/kV. The change in the slope beyond 10.2 kV is mainly due to the effect of a large noise rate. The fitted  $\sigma_{pos}$  and  $\sigma_{time}$  as a function of the applied voltage for the RPC under study is shown in Figs. 9 (b) and (c). The variation in the position resolution with different applied voltage shows improving behaviour

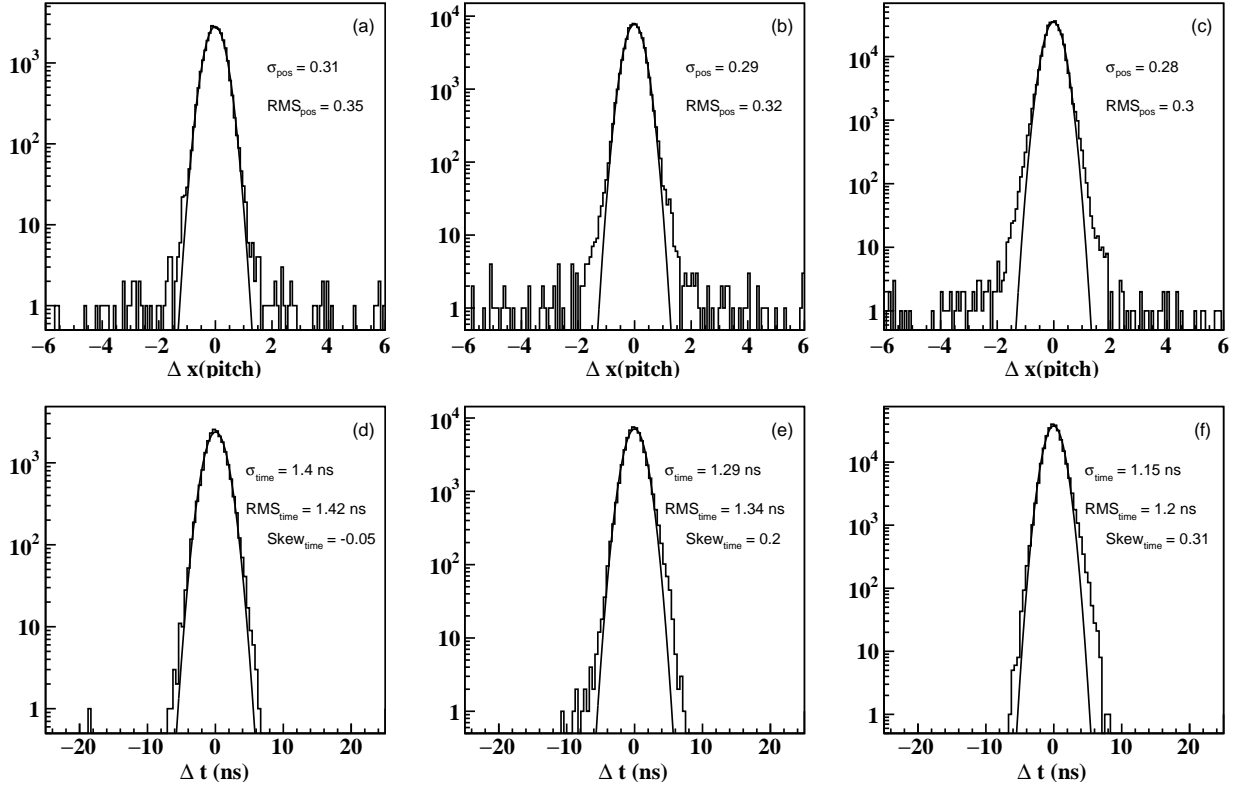


**Figure 8.** (a), (b) and (c) are the position residue distribution at 9.8 kV for efficiency zones of 20-30 %, 50-60 % and 80-90 % respectively. (d), (e) and (f) are the time residue distribution at 9.8 kV for efficiency zones of 20-30 %, 50-60 % and 80-90 % respectively.

upto  $\text{HV}_{\text{pos}}^{\text{min}} = 9.8\text{-}9.9 \text{ kV}$ . But beyond the  $\text{HV}_{\text{pos}}^{\text{min}}$ , the position resolution is deteriorating due to the increased contribution of the multiplicities which results in the poor localisation of the signal. The time resolution of the RPC under the study improves as the applied voltage increases upto  $\text{HV}_{\text{time}}^{\text{min}} = 10.4 \text{ kV}$ . The larger applied voltage above  $\text{HV}_{\text{time}}^{\text{min}}$  shows an increase in the time resolution. During each avalanche, even for the noise pulse, the effective high voltage at the avalanche position (few  $\text{mm}^2$ ) is reduced below the threshold voltage to form an avalanche signal, which causes the inefficiency as seen in the inset plot of Fig. 4(a) and gradually the high voltage is built up in that region. During the recovery time, the time taken by the system to regain its stable voltage configuration, the effective HV is low and consequently the gain is also low. This explains the change in slope in Figs. 9 (a) and increase of resolution in Figs. 9 (c). This argument is supported by the time residues distribution in the larger HV samples. Figs 10 (a), (b) and (c) are the time residue distribution for the efficiency zone of 50-60 % for 10.2 kV, 10.4 kV and 10.6 kV respectively. The time residue distribution for larger HV has an increasing number of events in the right side bump (which is small signals that cross the discriminator threshold later than the muon trigger time) and has increasing skewness at a larger voltage in comparison of skewness in Fig. 8(d) to Fig. 8(f).

The results of selected efficiency, as well as the position resolution, suggests that the optimum operating point of this RPC is 9.8-9.9 kV, not the 10.1-10.2 kV, which was obtained using the

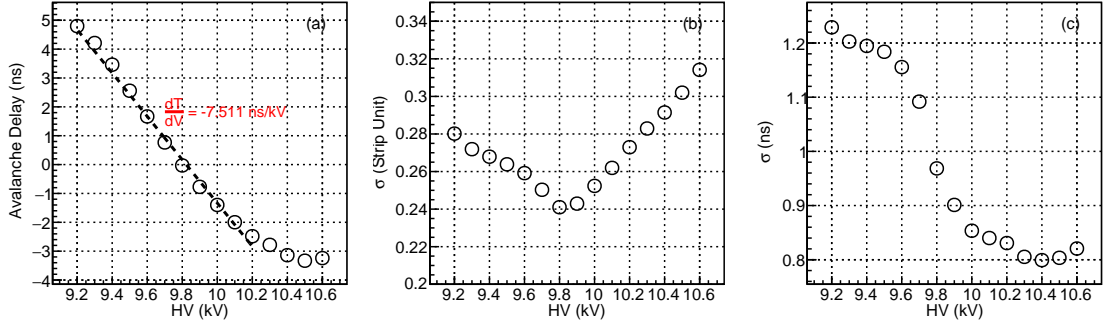


**Figure 9.** (a) is the mean of the time residues as a function of applied HV. (b) and (c) are the position and time resolution as a function of the applied voltage.

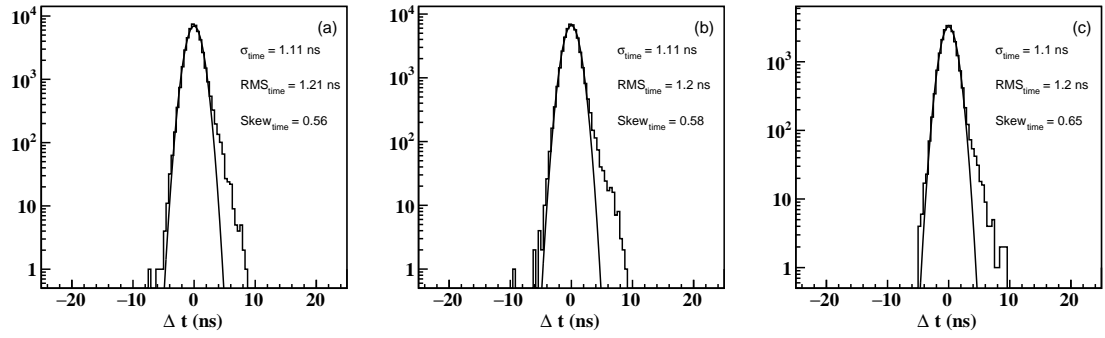


**Figure 10.** (a), (b) and (c) are the time residue distribution for the efficiency zone of 50-60 % for 10.2, 10.4 and 10.6 kV.

standard efficiency plots.

Another RPC, of non-uniform gain, is also studied in the same manner. The default efficiency and selected efficiency are shown in Figs. 11(a) and (b). Fig. 12(a) is the mean of the time residue as a function of HV is fitted using a straight line and the obtained slope for one of the planes is -6.21 ns/kV. The position resolution and time resolution at different operating voltages are shown in Figs. 12(b) and (c) respectively. That also shows that the optimum operating HV of the RPC for the best physics performance is obtained at ~9.8 kV, not 10.1-10.2 kV, which is obtained from the plateau of default efficiency.

## 8 Conclusion

Two RPCs were tested at different operating HV to choose the optimum operating HV for the best physics performance of the system. Due to the non-uniform response of these RPCs over the whole surface area, different regions show the saturation of efficiencies at different HV. Different zones can be considered as different individual RPCs, which should have different optimum operating HV. Though the plateau of efficiency apparently shows a larger operating voltage in terms of uniform gain, the optimum operating HV for the best performance of the detector is lower than that. This paper shows examples of two RPCs with large non-uniformities in gain. In general, these kinds

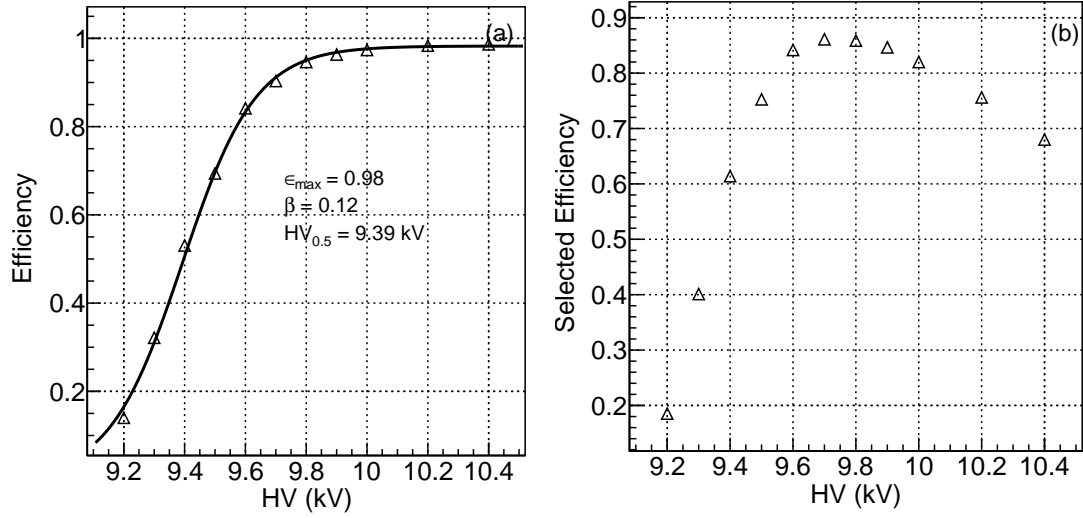


**Figure 11.** (a) and (b) are the default efficiency and selection efficiency as a function of applied HV for another RPC.

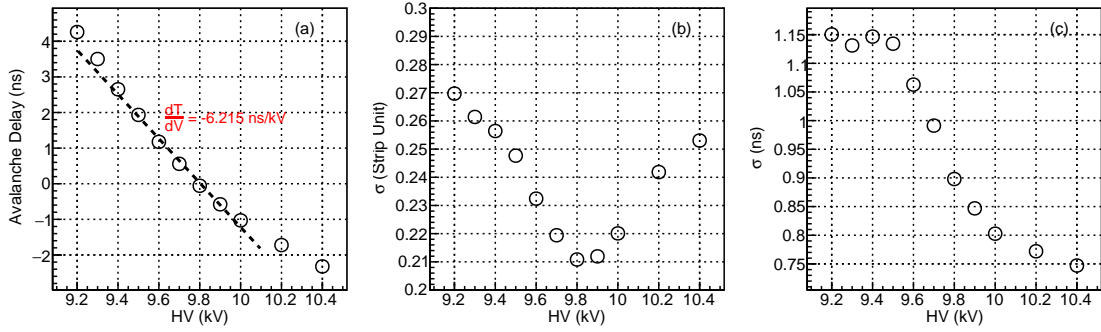


**Figure 12.** (a) is the mean of the time residues as a function of applied HV. (b) and (c) are the position and time resolution as a function of the applied voltage.

of chambers is not installed in an experiment. But, even one installs a good RPC in beginning, during the operational phase, characteristics of the RPC might change, e.g. change in resistivity in the graphite coating, bulging due to button popup etc., and then certainly one needs to check the optimum operating HV for the best physics out of it, not simple efficiency plateau. Even with a small variation of gain in an RPC, one should choose the operating HV by optimising the selected efficiency, resolutions but not only overall efficiency.

## Acknowledgments

We would also like to thank all members of the INO collaboration for their valuable inputs.



## References

- [1] ICAL Collab., S. Ahmed *et. al.*, *Physics Potential of the ICAL detector at the India-based Neutrino Observatory (INO)*, *Pramana* **86** (2017) 55.
- [2] R. Santonico, R. Cardarelli, *Development of resistive plate counters*, *Nucl. Instrum. Methods* **187** (1981) 377–380.
- [3] H. Raether, *The development of electron avalanche in a spark channel (from observations in a cloud chamber)*, *Z. Phys* **112** (1939) 464.
- [4] J.M. Meek, *A theory of spark discharge*, *Phys. Rev.*, **57** (1940) 722.
- [5] Gobinda Majumder, Suryanaraya Mondal *et. al.*, *Design, construction and performance of magnetised mini-ICAL detector module*, *PoS ICHEP2018* (2019) 360.
- [6] F. Anghinolfi *et al.* *NINO: an ultra-fast and low-power front-end amplifier/discriminator ASIC designed for the multigap resistive plate chamber*, *Nucl. Instrum. Methods A* **533** (2004) 183-187.
- [7] M. Abbrescia *et. al.*, *Beam test results on double-gap resistive plate chambers proposed for CMS experiment*, *Nucl. Instr. Meth. Phys. Res.* **A414** (1998) 135-148.
- [8] S. Pethuraj *et. al.*, *Measurement of azimuthal dependent muon flux by 2 m×2 m RPC stack at IICHEP-Madurai*, *Experimental Astronomy* **49** (2020) 141-147.
- [9] G. Majumder, N.K. Mondal, S. Pal, D. Samuel, B. Satyanarayana *Study of the directionality of cosmic muons using the INO-ICAL prototype detector*, *Nucl. Instr. Meth. Phys. Res.* **A735** (2014) 88-93.
- [10] A.D. Bhatt, G. Majumder, N.K. Mondal, Pathaleswar, B. Satyanarayana *Improvement of time resolution in large area single gap Resistive Plate Chambers*, *Nucl. Instr. Meth. Phys. Res.* **A844** (2017) 53-61.
- [11] CMS HCAL/ECAL Collaborations, *The CMS barrel calorimeter response to particle beams from 2 to 350 GeV/c*, *Eur. Phys. J.* **C60** (2009) 359-373.
- [12] S. Costantini on behalf of the CMS Collaboration, *Calibration of the RPC working voltage in the CMS experiment*, CMS CR 055 (2012). DOI: <https://doi.org/10.22323/1.159.0005>.
- [13] B. Bartoli *et al.* *Study of RPC gas mixtures for the ARGO-YBJ experiment*, *Nuclear Instruments and Methods in Physics Research A* **456** (2000) 35-39.